Brazilian Journal
of Chemical
Engineering

ISSN 0104-6632
Printed in Brazil
www.abeq.org.br/bjche

Vol. 36, No. 03, pp. 1075 - 1087, July - September, 2019
dx.doi.org/10.1590/0104-6632.20190363s20180588

DENSITY CALCULATIONS OF AQUEOUS AMINE SOLUTIONS USING AN EXCESS GIBBS BASED MODEL

Diego D. D. Pinto[1,2*] and Hanna K. Knuutila[1]

[1] Norwegian University of Science and Technology, Department of Chemical Engineering, Trondheim, Norway.
E-mail: diego.pinto@hovyu.com - ORCID: 0000-0001-5381-1163; ORCID: 0000-0003-2057-1743
[2] Hovyu B.V., Alphen aan den Rijn, Netherlands.

(Submitted: December 10, 2018 ; Revised: April 2, 2019 ; Accepted: April 5, 2019)

Abstract - Accurate representation of the physical properties of a solvent is essential for design and simulation of processes. Density and viscosity, for instance, have an important role in modelling and designing absorption and desorption towers. In the present work, a model to accurately calculate the density of aqueous amine solutions used in CO_2 capture was developed as a function of temperature and composition. The model is based on excess Gibbs energy functions, and in this work the functional form of the non-random two-liquid (NRTL) model was used. The model is able to accurately represent the density of the tested systems with deviations below 0.2% for most cases. The pure component density was calculated using the modified Rackett equation with the parameter Z_{RA} as a function of the temperature and pressure of the system. The calculated deviation (AARD) for pure component density was below 0.09%.
Keywords: Density; CO_2 capture; Amine; Multicomponent; Modified Rackett.

INTRODUCTION

In the context of CO_2 removal from gas streams, absorption processes with alkanolamines are the state of the art (Bernhardsen et al., 2018) and monoethanolamine (MEA) is considered the benchmark solvent. One of the major disadvantages of post-combustion capture processes is the process energy requirements. The state of the art MEA is known to require 3.4-4 GJ/ton CO_2 (Liebenthal et al., 2013; Kvamsdal et al., 2011; Knudsen et al., 2009, 2007). However, some new solvents are claimed to reduce the regeneration energy requirement. For instance, Pinto et al. (2014a) showed that, using an aqueous solution of DEEA/MAPA as a solvent, it was possible to achieve a reboiler duty of 2.2-2.4 GJ/ton CO_2.

Accurate representation of the physical properties of a solvent is essential for design and simulation of processes. Razi et al. (2012) reviewed the impact of using different correlations in the design of CO_2 capture plants using MEA as a solvent. They pointed out the uncertainties related on applying some of the correlations. It is evident that a good description on the behaviour of the solvent is very important. Physical properties like density and viscosity have an important role in modelling and designing of absorption and desorption towers due to the significant influence on the mass transfer coefficient, kinetics and hydrodynamic behaviour (Gao et al., 2017; Àlvarez et al., 2006).

In the present work, a model to accurately calculate the density of liquid mixtures was developed. The model is based on excess Gibbs energy functions and, in this work, the functional form of the non-random two-liquid (NRTL) model (Renon and Prausnitz, 1968) was used. The model was tested focusing on solvents used in CO_2 capture processes. Seven systems were tested (5 binaries and 2 ternaries) in which it was possible to check the model capacity to accurately calculate their density. Moreover, the pure component density was calculated using the modified Rackett

* Corresponding author: Diego D. D. Pinto - E-mail: diego.pinto@hovyu.com

equation with the parameter Z_{RA} as a function of the temperature and pressure of the system.

LITERATURE REVIEW

Several attempts to model the density of a pure component have been used in the literature. Yang et al. (2012) and Pinto et al. (2014b) used a second order temperature polynomial model (Eq. 1), while Muhammad et al. (2009) used a simple linear correlation (Eq. 1 with parameter c = 0).

$$\rho_i = a + bT + cT^2 \tag{1}$$

Mokraoui et al. (2006) and Rayer et al. (2010) used an empirical correlation (Eq. 2) to calculate the density of pure components. In this correlation, A, B and C are adjustable parameters, MW_i is the molecular weight of the component and T_r is the reduced temperature.

$$\rho_i = \frac{A}{B^{\left(1+(1-T_r)^C\right)}} \frac{MW_i}{1000} \tag{2}$$

The Rackett equation is commonly used to represent the molar volumes of saturated liquids ($\overline{V_i}$). However, this equation has no adjustable parameters. To allow extra flexibility to Rackett's model, the critical compressibility factor was exchanged to the Rackett compressibility factor (Z_{RA}) which is fitted to experimental data. This variant of the Rackett equation is often called the modified Rackett equation and it is presented in Eq. 3, where R, T_c and p_c are, respectively, the universal gas constant, the critical temperature and the critical pressure.

$$\overline{V_i} = \left(\frac{RT_c}{p_c}\right) Z_{RA}^{\left(1+(1-T_r)^{2/7}\right)} \tag{3}$$

The density can then be easily calculated from the molar volume (Eq. 4).

$$\rho_i = \frac{MW_i}{\overline{V_i}} \tag{4}$$

Pinto et al. (2014b) also used the modified Rackett equation to model the pure component liquid density. In that work, Z_{RA} was fitted as a constant for all range of temperature. As Z_{RA} is a fitted parameter, many authors have proposed different forms to describe this parameter (Vetere, 1992; Campbell and Thodos, 1984). In this work, the modified Rackett equation (Eq. 3) was used to calculate the density of the pure component with the Z_{RA} as given in Eq. 5, where A, B and C are adjustable parameters and p_r is the reduced pressure.

$$Z_{RA} = \exp\left(A + \frac{B}{p_r} + C \cdot \ln\left(T_r\right)\right) \tag{5}$$

Liquid mixture density models

Henni et al. (2003) and Chowdhury et al. (2009) correlated the densities of several binary aqueous amine solutions using a polynomial function (Eq. 6). Although the correlation is very accurate, the model does not take into account the temperature dependency. The optimization had to be carried out for each temperature and each component, and calculations at temperatures different from the optimized are not readily available. Moreover, the number of polynomial terms (parameters) can vary considerably. In the mentioned works, the authors chose 5-6 parameters per temperature.

$$\rho = \sum_{i=1}^{n} a_i \cdot x_1^i \tag{6}$$

Àlvarez et al. (2006) proposed an equation similar to the Grunberg-Nissan equation (Gunberg and Nissan, 1949) (Eq. 7) to correlate the density of ternary systems (water plus 2 amines). They used 3 parameters to correlate the density of the ternary systems. However, as in Chowdhury et al. (2009), the model has no temperature dependency. Moreover, the binary interaction parameter (A_{ij}) was estimated for each temperature. One great disadvantage of the model presented in Eq. 7 is not being able to calculate the density of the solution at different temperatures with a unique set of parameters.

$$\rho = \sum_{i=1}^{3} x_i \rho_i + \sum_{i \neq j} A_{ij} x_i x_j \tag{7}$$

One common approach to model the density of liquid mixtures is through the excess molar volume (Eq. 8) where $\overline{V^E}$, $\overline{V^m}$ and $\overline{V_i^0}$ are, respectively, the excess, mixture and pure component molar volumes and x_i is the mol fraction of component *i*. By using this approach, it is possible to regress to the smaller subsystems maintaining good accuracy in the calculations. Similar approaches have been used to correlate viscosity (Pinto et al., 2017; Pinto and Svendsen, 2015).

The molar volumes, however, can be written in terms of the densities (ρ) and component molecular weights (MW), according to Eq. 9. After some manipulation of Eq. 9, the density of a liquid mixture can be expressed as a function of the pure component densities, the molecular weights and the excess molar

volume (Eq. 10). There is a variety of ways to represent mathematically the molar excess volume. The Redlich-Kister model (Redlich and Kister, 1948), nevertheless, is very often used for this purpose. The Redlich-Kister model is a simple correlation based on a polynomial series and, for a binary system, is expressed in Eq. 11. The number of parameters is variable and dependent on the order of the polynomial. Although the expansion of the Redlich-Kister to multicomponent systems is not difficult, the number of parameters is significantly increased.

$$\overline{V^E} = \overline{V^m} - \sum_{i=1}^{NC} x_i \overline{V_i^0} \tag{8}$$

$$\overline{V^E} = \frac{\sum_{i=1}^{NC} x_i MW_i}{\rho} - \sum_{i=1}^{NC} \frac{x_i MW_i}{\rho_i} \tag{9}$$

$$\rho = \frac{\sum_{i=1}^{NC} x_i MW_i}{\overline{V^E} + \sum_{i=1}^{NC} \frac{x_i MW_i}{\rho_i}} \tag{10}$$

$$\overline{V^E} = x_1 x_2 \sum_{i=1}^{NP} A_i (x_1 - x_2)^i \tag{11}$$

Many authors used the Redlich-Kister correlation to model the excess molar volume of liquid mixtures at specific temperatures (Zhang et al., 1995; Maham et al., 1995; Alvarez et al., 2010). Although this approach generates accurate correlations, there is a need for a set of parameters per temperature of interest. Moreover, there is no continuity (with respect to temperature) and the calculation outside the optimized conditions is not straightforward. Several authors attempted to solve this problem by creating a temperature dependency for the Redlich-Kister parameter (A_i) as for instance in Pinto et al. (2014b) (Eq. 12). With this approach, the calculation of the density at temperatures different than the ones used for the parameter estimation can be achieved with a unique set of optimized parameters.

$$A_i = a_i + b_i T \tag{12}$$

The Redlich-Kister model has the same drawback as the models based on polynomial series. The number of parameters is user-defined and can be significantly high. It is commonly reported (Maham et al., 1995; Zhang et al., 1995) that at least 6 parameters per temperature are required to model liquid densities when using the Redlich-Kister model. The total number of parameters estimated by Maham et al. (1995) to model the density of aqueous MDEA solutions for the whole range of composition and at 7 temperatures was 42. Han et al. (2012b) and Pinto et al. (2014b), applied a temperature dependency on the regressed parameter and reduced the number of total parameters for the aqueous MEA systems to 8 and 6, respectively. Although the implementation of the temperature dependency drastically reduced the total number of estimated parameters, this number is still considered high for a binary system.

MULTICOMPONENT DENSITY MODEL BASED ON EXCESS GIBBS ENERGY MODELS

Excess Gibbs energy models, for instance the NRTL (Renon and Prausnitz, 1968), UNIQUAC (Abrams and Prausnitz, 1975) and Wilson (Wilson, 1964), are well known and widely used models. Recently, Pinto and Svendsen (2015) showed that excess Gibbs energy models could be used to represent the viscosity of liquid solutions. The excess Gibbs energy model was used to represent an "excess viscosity" term.

The excess molar volume follows a similar shape as the excess molar Gibbs energy (Figure 1). Therefore, it is presumable that well-established excess Gibbs energy models could as well be used to represent this quantity.

The use of models such as the NRTL to represent the excess molar volume would limit the number of adjustable parameters, as well as allow directly interpolation, as they are continuous functions of temperature and composition. The NRTL model is used in this work to represent the excess property as given in Eqs. 13-15. However, any of the other models (for example, UNIQUAC or Wilson) could be used with the same accuracy expected. In this work the parameter R is fixed at 8.314. The temperature, pressure and molecular weights are given in K, MPa

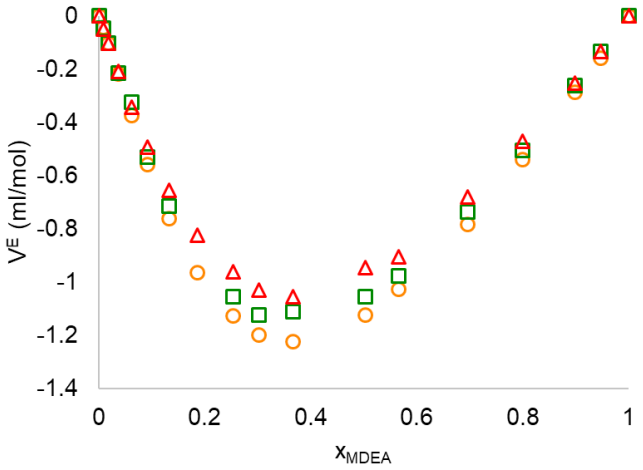

Figure 1. Excess volume of MDEA as a function of mol fraction at: (O) 303.15 K, (□) 323.15 K and (Δ) 323.15. Experimental data from (Maham et al., 1995).

and g/mol, respectively, while the calculated densities are given in g/ml.

$$\overline{V^E} = RT\sum_{i=1}^{NC} x_i \frac{\sum_{j=1}^{NC}\tau_{ji}G_{ji}x_j}{\sum_{k=1}^{NC}G_{ki}x_k} \quad (13)$$

$$G_{ij} = \exp\left(-\alpha_{ij}\tau_{ij}\right) \quad (14)$$

$$\tau_{ij} = a_{ij} + \frac{b_{ij}}{T} \quad ; \quad \tau_{ii} = 0 \quad (15)$$

OPTIMIZATION ROUTINE

As in previous works (Pinto et al., 2013, 2017; Monteiro et al., 2013), the particle swarm optimization (PSO) routine is used to estimate the parameters. The objective function used is given in Eq. 16. The absolute average relative deviation (AARD), the absolute average deviation (AAD) and the maximum absolute deviation (MAD), given, respectively, through Eqs. 17-19, were used to measure the deviation between the calculated and experimental density.

The optimization was carried using the sequential optimization procedure where the smaller subsystems were optimized first and their parameters carried forward to the next optimization. As an example, for the ternary system H_2O-MEA-MDEA, the first optimization was the pure densities using the modified Rackett equation. These parameters were later used in the optimization of the binary systems (H_2O-MEA and H_2O-MDEA), which generated interaction parameters water-amine. The binary parameters were carried to the ternary system optimization (H_2O-MEA-MDEA) where the only parameters optimized were related to the MEA-MDEA interaction.

By using this procedure, it is ensured that, in the case of an absence of one of the components the system will regress to the smaller subsystem with the same accuracy as they were optimized. For instance, if the MDEA mole fraction is set to zero (absence of MDEA) in the H_2O-MEA-MDEA system, the model will calculate the binary system (H_2O-MEA) with the same accuracy as that with which binary system was optimized.

$$F_{obj.} = \sum_{i=1}^{N} \frac{\left(y_i^{exp.} - y_i^{cal.}\right)^2}{y_i^{exp.} y_i^{cal.}} \quad (16)$$

$$AARD(\%) = \frac{100}{N}\sum_{i=1}^{N} \frac{\left|y_i^{exp.} - y_i^{cal.}\right|}{y_i^{exp.}} \quad (17)$$

$$AAD(g/ml) = \sum_{i=1}^{N} \frac{\left|y_i^{exp.} - y_i^{cal.}\right|}{N} \quad (18)$$

$$MAD(g/ml) = \max\left(\left|y_i^{exp.} - y_i^{cal.}\right|\right) \quad (19)$$

Three optimizations were performed where the non-randomness parameter (α_{ij}) was fixed at 0.1, 0.2 and 0.3. The objective function values were most of the time similar, independent of the non-randomness parameters used.

RESULTS

Seven systems were selected to test the proposed model. The components and their properties are presented in Table 1. The modified Rackett equation (Eqs. 3, 4, and 5) is used to model the pure substance density. In this work, the density is given in g/ml, the temperature in K and the pressure in MPa. In Table 2, the optimized parameters for the modified Rackett equation are given whereas Table 3 presents the calculated deviations. It is seen that the Rackett equation is able to provide accurate calculations for the liquid density, except in the region close to the fusion point for water. Nevertheless, these deviations are within a reasonable acceptable range. The calculated deviations are small and the model is able to represent the data well.

In Table 4, the optimized parameters for the aqueous systems are given and the deviations are found in Table 5. From Table 4, it is seen that, with few exceptions, the parameters present an antisymmetric behaviour (Eq. 20). Parameter a_{ij} seems to have this behaviour

Table 1. Studied components and its respective properties (Yaws, 2012).

Component	CAS	MW (g/mol)	p_c (MPa)	T_c (K)
H_2O	7732-18-5	18.02	22.064	647.10
MEA	141-43-5	61.08	8.03	671.40
MDEA	105-59-9	119.16	3.88	675.00
AMP	124-68-5	89.14	4.14	571.82
DEA	111-42-2	105.14	4.27	736.60
PZ	110-85-0	86.14	5.53	638.00

Table 2. Modified Rackett parameters for calculating pure component density (ρ in g/ml, T in K and p in MPa).

Component	A	B	C
H_2O	-1.4937	6.6495E-06	-9.868E-02
MEA	-1.3383	1.5740E-05	-1.572E-02
MDEA	-1.3997	6.0751E-05	-3.240E-02
AMP	0.1279	-3.7692E-02	-6.1425E-02
DEA	-3.0305	3.6589E-02	-4.1276E-02
PZ[a]	-1.1301	0	0

[a] ZRA = Zc.

Table 3. Calculated deviations for pure component density.

Component	AARD (%)	AAD (kg/m^3)	MAD (kg/m^3)	Source
H_2O	0.346	3.044	15.821	Wagner and Pruß (2002)
MEA	0.015	0.152	0.209	Amundsen et al. (2009)
	0.085	0.871	1.310	Maham et al. (2002)
	0.076	0.761	1.647	Hawrylak et al. (2000)
	0.047	0.457	1.139	Han et al. (2012b)
	0.047	0.464	1.647	Total
MDEA	0.092	0.950	1.358	Hawrylak et al. (2000)
	0.052	0.523	0.873	Maham et al. (1995)
	0.033	0.336	0.859	Pinto et al. (2014b)
	0.062	0.601	2.453	Han et al. (2012a)
	0.028	0.294	0.715	Chowdhury et al. (2009)
	0.054	0.542	2.453	Total
AMP	0.052	0.468	0.615	Henni et al. (2003)
	0.050	0.453	0.834	Xu et al. (1991)
	0.047	0.426	0.515	Chan et al. (2002)
	0.050	0.450	0.834	Total
DEA	0.036	0.387	1.065	Hawrylak et al. (2000)
	0.020	0.212	0.341	Chowdhury et al. (2009)
	0.020	0.219	0.361	Maham et al. (1994)
	0.018	0.191	0.530	Yang et al. (2012)
	0.022	0.234	1.065	Total

for all systems with the exception of PZ systems. An optimization using the antisymmetric approach (Eq. 20) was performed for parameters for H_2O-MDEA system ($a_{H_2O,MDEA}$ = 0.01396, $b_{H_2O,MDEA}$ = -36.997 and $\alpha_{H_2O,MDEA}$ = 0.2). The AARD, AAD and MAD were, respectively, 0.29%, 2.97 kg/m^3 and 13.4 kg/m^3. This result was not as accurate as when using the decoupled parameters, where the deviations were calculated as 0.093%, 0.941 kg/m^3 and 10.499 kg/m^3. Therefore, it was decided not to use the antisymmetric approach.

Table 5. Calculated deviations for aqueous amine system density.

System	AARD (%)	AAD (kg/m^3)	MAD (kg/m^3)	Source
H_2O-MEA	0.086	0.866	2.594	Amundsen et al. (2009)
	0.176	1.788	4.138	Maham et al. (2002)
	0.109	1.102	9.281	Hawrylak et al. (2000)
	0.087	0.869	1.957	Li and Lie (1994)
	0.082	0.805	2.124	Han et al. (2012b)
	0.102	1.023	9.281	Total
H_2O-MDEA	0.110	1.134	10.499	Hawrylak et al. (2000)
	0.056	0.564	1.000	Li and Lie (1994)
	0.084	0.857	8.669	Maham et al. (1995)
	0.063	0.643	2.246	Pinto et al. (2014b)
	0.123	1.223	3.590	Han et al. (2012a)
	0.050	0.519	1.383	Chowdhury et al. (2009)
	0.093	0.941	10.499	Total
H_2O-AMP	0.076	0.728	1.802	Henni et al. (2003)
	0.114	1.092	3.284	Xu et al. (1991)
	0.078	0.752	2.079	Chan et al. (2002)
	0.084	0.806	3.284	Total
H_2O-PZ	0.053	0.526	1.277	Samanta and Bandyopadhyay (2006)
	0.066	0.659	1.522	Derks et al. (2005)
	0.036	0.357	0.784	Sun et al. (2005)
	0.077	0.761	1.669	Muhammad et al. (2009)
	0.060	0.602	1.669	Total
H_2O-DEA	0.040	0.426	1.577	Hawrylak et al. (2000)
	0.074	0.786	1.494	Chowdhury et al. (2009)
	0.045	0.469	1.723	Maham et al. (1994)
	0.050	0.525	3.084	Yang et al. (2012)
	0.050	0.530	3.084	Total
H_2O-MEA-MDEA	0.062	0.617	1.957	Li and Lie (1994)
	0.033	0.326	0.975	Li and Shen (1992)
	0.091	0.924	1.864	Hagewiesche et al. (1995)
	0.050	0.502	1.232	Hsu and Li (1997)
	0.056	0.561	1.957	Total
H_2O-MDEA-PZ	0.205	2.089	6.799	Paul and Mandal (2006)
	0.184	1.889	4.714	Muhammad et al. (2009)
	0.193	1.974	6.799	Total

Table 4. Optimized parameters for calculating densities in aqueous systems.

i	j	a_{ij}	a_{ji}	b_{ij}	b_{ji}	$\alpha_{ij} = \alpha_{ji}$
H_2O	MEA	-0.0565	0.0575	-0.3610	-0.04512	0.2
H_2O	MDEA	-0.5022	0.5313	-26.5001	28.2631	0.1
H_2O	AMP	-0.2824	0.2821	-95.0253	105.9925	0.1
H_2O	PZ	-0.0056	109.0230	-3.2495	-21495.84	0.3
H_2O	DEA	-0.1475	0.1533	-21.7881	24.3958	0.3
MEA	MDEA	-0.2797	0.2421	-2.0375	21.2321	0.3
MDEA	PZ	25.5927	-0.4141	-2917.5751	-217.7676	0.2

By doing this, all systems were calculated with very low deviations (AARD below 0.2%).

$$a_{ij} = -a_{ji} \quad ; \quad b_{ij} = -b_{ji} \tag{20}$$

Water

The modified Rackett equation was used to model the density of pure water. Data from Wagner and Pruß (2002) were used for regressing the parameters. The data cover a broad range of temperatures and pressures (0.05 to 20 MPa). The model is able to represent the density of water at several temperatures and pressures. It is seen from Figure 2 that, at 101.325 kPa, the model presents a higher deviation at low temperature (close to the melting point). However, this deviation is below 1% and considered negligible for engineering calculations. At 101.325 kPa, the AARD, AAD and MAD are calculated to be 0.129%, 1.285 kg/m^3 and 5.171 kg/m^3. In fact, the majority of the data is calculated within 1% deviation.

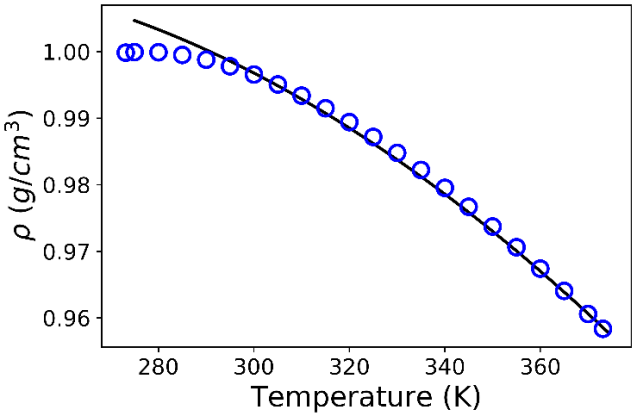

Figure 2. Density of pure water at 101.325 kPa. (-) model, (o) Wagner and Pruß (2002).

MEA

The modified Rackett equation was used to correlate the density of pure MEA as a function of temperature and pressure. For MEA, measurements at two different pressures were used, namely 101.325 and 700 kPa. The calculated deviations reported in Table 3 are very small, indicating a good agreement between the model and the experimental data. This is confirmed in Figures 3 and 4 where it is seen that the model is able to accurately represent the data at several temperatures at 101.325 kPa.

In Figure 6, the density of aqueous solutions of MEA for the whole range of concentration and at several temperatures are shown at 101.325 kPa. There are plenty of experimental data available for this system at atmospheric conditions. It is seen that the model is able to accurately calculate the density of aqueous MEA solutions at several different temperatures. At 700 kPa, however, the model slightly over predicts the

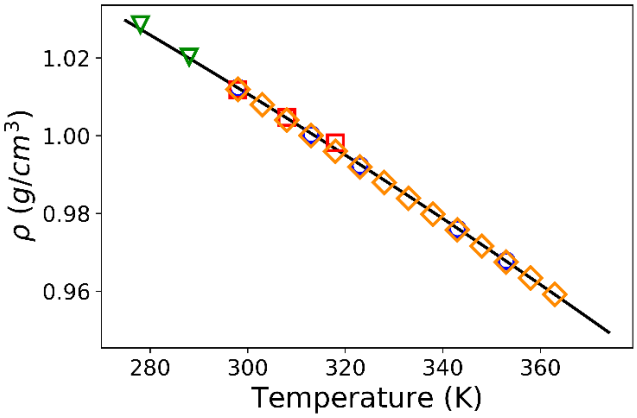

Figure 3. Density of pure MEA at different temperatures. Experimental data from: (o, Amundsen et al. (2009)), (∇, Maham et al. (2002)), (□, Hawrylak et al. (2000)) and (◊, Han et al. (2012b)). (-) model at 101.325 kPa.

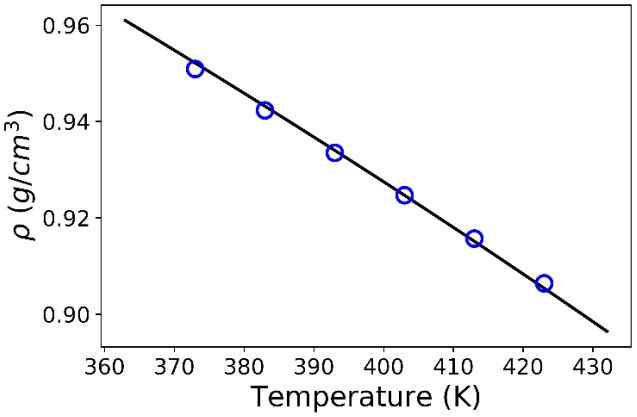

Figure 4. Density of pure MEA at different temperatures. Experimental data from: (o, Han et al. (2012b)). (-) model at 700 kPa.

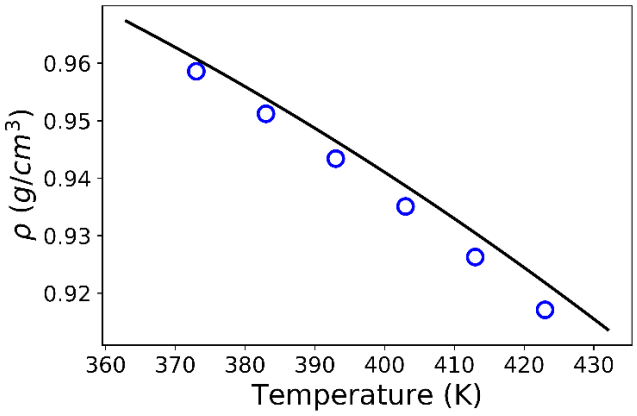

Figure 5. Density of pure water at different temperatures. Experimental data from: (o, Han et al. (2012b)). (-) model at 700 kPa.

density of pure water for all temperatures, as seen in Figure 5. This, evidently, makes the model predictions less accurate in the low amine concentration region, as seen in Figure 7. However, this can be fixed if a more

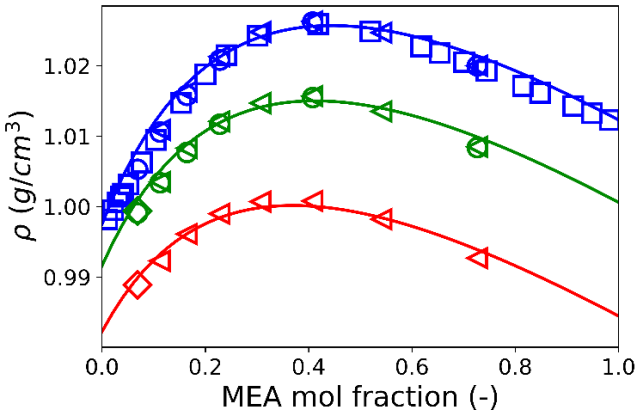

Figure 6. Density of aqueous MEA solution at different temperatures. Experimental data from: (o, Amundsen et al. (2009)), (◁, Han et al. (2012b)), (□, Hawrylak et al. (2000)), (◊, Li and Lie (1994)). Model at 101.325 kPa and (-, blue) 298.15 K, (-, green) 313.15 K and (-, red) 333.15 K.

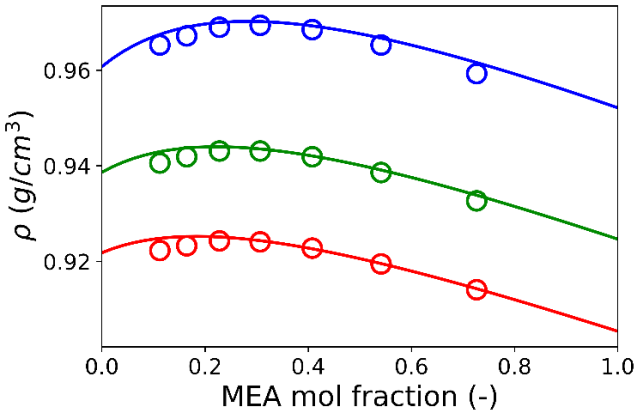

Figure 7. Density of aqueous MEA solution at different temperatures. Experimental data from: (o, Han et al. (2012b)). Model at 700 kPa and (-, blue) 373.15 K, (-, green) 403.15 K and (-, red) 423.15 K.

accurate model for water density is used, for example the model proposed in Wagner and Pruß (2002). Nevertheless, the deviations are acceptable and the overall calculations are quite accurate. The best fit for aqueous MEA solutions was achieved using $\alpha_{ij} = 0.2$.

MDEA

As for MEA, densities measured at two pressures and several temperatures were used for fitting the parameters for the MDEA density model. The same good fit is also seen for the density of pure MDEA (Figures 8 and 9). Figures 10 and 11 show the calculated and experimental densities of aqueous MDEA solutions at 101.325 and 700 kPa at several temperatures. Differently from MEA, the best fit was found with $\alpha_{ij} = 0.1$. It is important to note that the MAD for Hawrylak et al. (2000) and Maham et al. (1995) are large compared to other sources. This is due to outliers which can be clearly seen in Figure

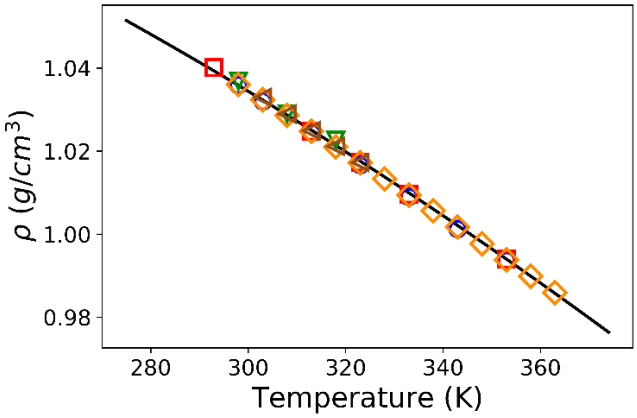

Figure 8. Density of pure MDEA at different temperatures. Experimental data from: (o, Maham et al. (1995)), (∇, Hawrylak et al. (2000)), (□, Pinto et al. (2014b)), (◊, Han et al. (2012a)) and (◁, Chowdhury et al. (2009)). (-) model at 101.325 kPa.

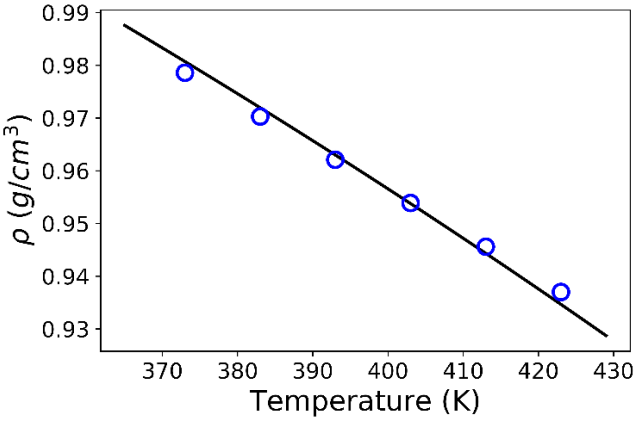

Figure 9. Density of pure MDEA at different temperatures. Experimental data from: (o, Han et al. (2012a)) and (-) model at 700 kPa.

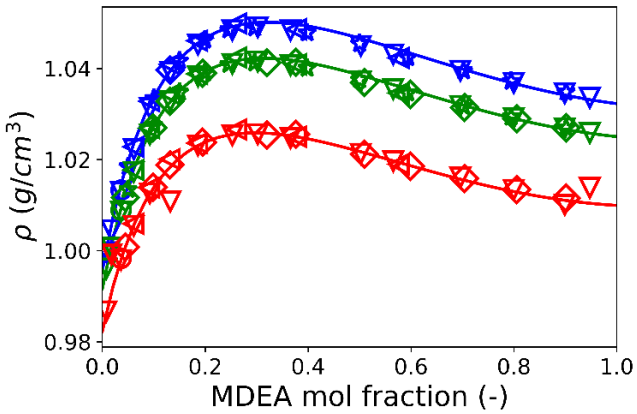

Figure 10. Density of aqueous MDEA solution at different temperatures. Experimental data from: (o, Li and Lie (1994)), (∇, Maham et al. (1995)), (◊, Pinto et al. (2014b)), (◁, Han et al. (2012a)) and (*, Chowdhury et al. (2009)). Model at 101.325 kPa and: (-, blue) 303.15 K, (-, green) 313.15 K and (-, red) 333.15 K.

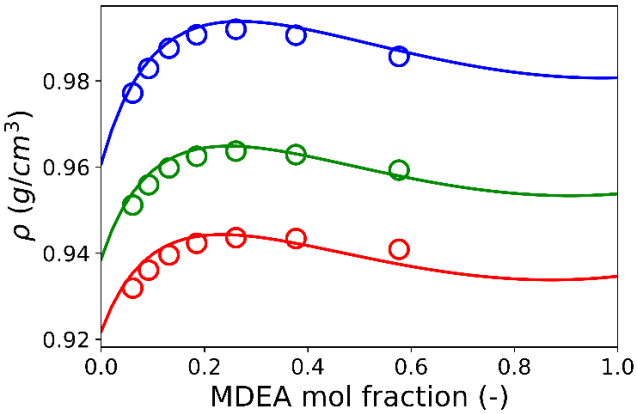

Figure 11. Density of aqueous MDEA solution at different temperatures. Experimental data from: (o, Han et al. (2012a)). Model at 700 kPa and: (-, blue) 373.15 K, (-, green) 403.15 K and (-, red) 423.15 K.

10 at 333 K and 0.018 and 0.13 MDEA mol fraction regarding data from Maham et al. (1995). The outlier in the data from Hawrylak et al. (2000) occurs at 308.15 K and 0.06 MDEA mol fraction. It is not clear whether it was a measurement or a reporting issue. However, in this work, it was decided to use the data as reported by the authors without excluding any data points. Disregarding these points, the calculated deviations are very small, indicating a good fit.

AMP

The density of pure AMP as a function of temperature is shown in Figure 12. It is seen that the model accurately represents the experimental data. The AARD is calculated below 0.06%, indicating not only good accuracy from the model, but also a good agreement between the dierent experimental sources. It should be noted, however, that AMP is solid at room temperature (the melting point is around 31 ºC (PubChem, 2018a)). Nevertheless, the model calculates a "virtual" density for temperatures lower than the melting point. This model should be used with care as prediction of phase changes is not possible. For the aqueous solutions at temperatures below the AMP melting point, the modified Rackett equation was still used to calculate the density of pure AMP as if it was a liquid.

For aqueous AMP solutions, the best set of parameters to describe the density as a function of temperature was found using α_{ij} = 0.1. Once again, the model is able to accurately predict the density of aqueous solutions at several temperatures (Figure 13).

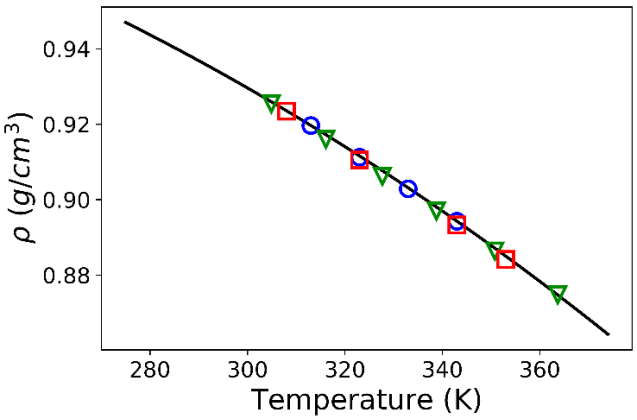

Figure 12. Density of pure AMP at different temperatures. Experimental data from: (o, Henni et al. (2003)), (∇, Xu et al. (1991)), (□, Chan et al. (2002)), (◊, Han et al. (2012a)) and (◃, Chowdhury et al. (2009)). () model at 101.325 kPa.

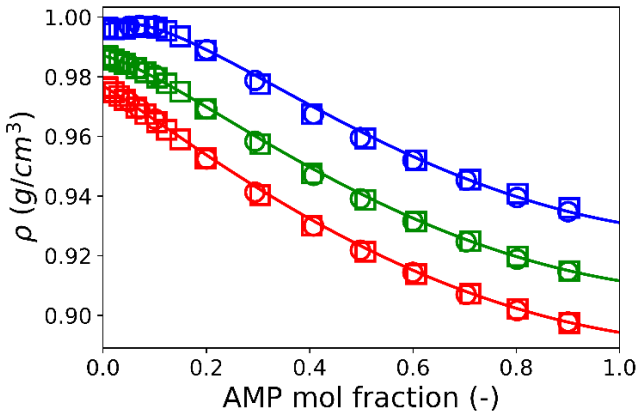

Figure 13. Density of aqueous AMP solution at different temperatures. Experimental data from: (o, Henni et al. (2003)) and (□, Chan et al. (2002)). Model at 101.325 kPa and:(-, blue) 298.15 K, (-, green) 323.15 K and (-, red) 343.15 K.

DEA

The modified Rackett equation was able to calculate the density of pure DEA with great accuracy as shown in Figure 14. As for AMP, DEA is solid at room temperature (melting point around 28 ºC). The

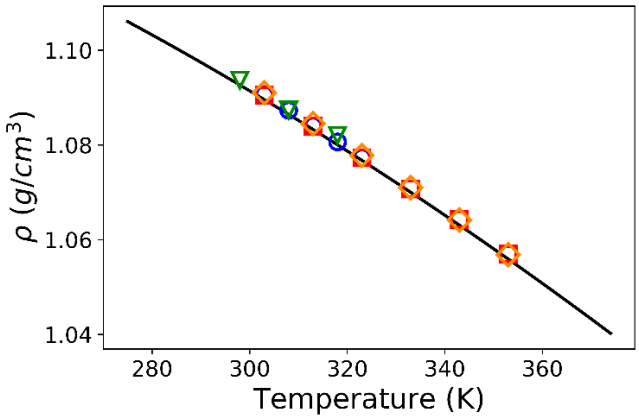

Figure 14. Density of pure DEA at different temperatures. Experimental data from: (o, Chowdhury et al. (2009)), (∇, Hawrylak et al. (2000)), (□, Maham et al. (1994)) and (◊, Yang et al. (2012)). (-) model at 101.325 kPa.

modified Rackett is not able to predict phase changes and the densities calculated for DEA at temperatures below 28 ºC are "virtual" liquid densities. For the aqueous system at temperatures below the melting point, the density of pure DEA is calculated using the modified Rackett equation as if DEA was a liquid at those conditions, like was done for AMP.

Figure 15 shows the density of the aqueous DEA system at several temperatures. Also there it is possible to see the good agreement between the model and the experimental data. The calculated deviations were also very low. The best fit was achieved with $\alpha_{ij} = 0.3$.

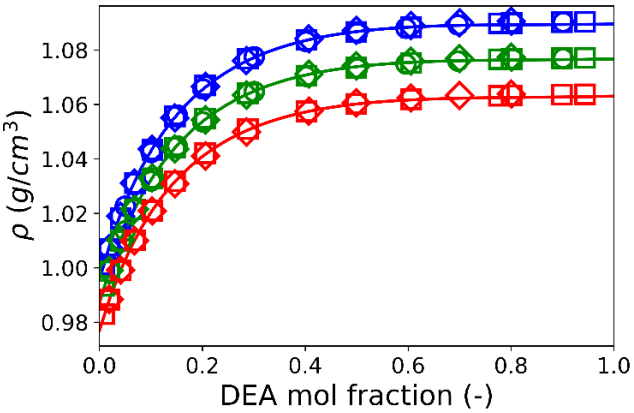

Figure 15. Density of aqueous DEA solution at different temperatures. Experimental data from: (o, Chowdhury et al. (2009)), (□, Maham et al. (1994)) and (◊, Yang et al. (2012)). Model at 101.325 kPa and: (-, blue) 303.15 K, (-, green) 323.15 K and (-, red) 343.15 K.

PZ

As for AMP and DEA, PZ is solid at room temperature (melting point is 106 ºC (PubChem, 2018b)). However, no data was found for the density of pure PZ. At temperatures above the melting point. In this case, for calculating the density of pure component it was considered that Z_{RA} equals the Z_c and the modified Rackett equation would regress to the original Rackett equation.

PZ has an additional solubility issue in aqueous solution as it can precipitate depending on the temperature and concentration. As the model cannot predict any phase change behaviour, some care should be taken when using it. The data from the literature is limited to PZ mol fractions lower than 0.04 (16.6 wt.%). A little scatter is also seen in the experimental data which was not seen for other systems. Nevertheless, the model is able to represent the experimental data accurately enough given the scatter in the experimental data, as seen in Figure 16. In this case, $\alpha_{ij} = 0.3$ provided the best set of parameters.

H_2O-MEA-MDEA

After having estimated the parameters of the density models to calculate the density of pure water, pure MEA, pure MDEA, aqueous MEA and aqueous MDEA, those parameters were carried forward for the optimization of the ternary H_2O-MEA-MDEA system. As a result, only four parameters were optimized ($a_{MEA,MDEA}$, $a_{MDEA,MEA}$, $b_{MEA,MDEA}$, $b_{MDEA,MEA}$). The results are given in Table 4. The calculated deviations were very small, as seen in Table 5. The parity plot (Figure 17) shows that all data lies across the diagonal line, which indicates a very good accuracy of the model. The best fit was obtained with $\alpha_{ij} = 0.3$.

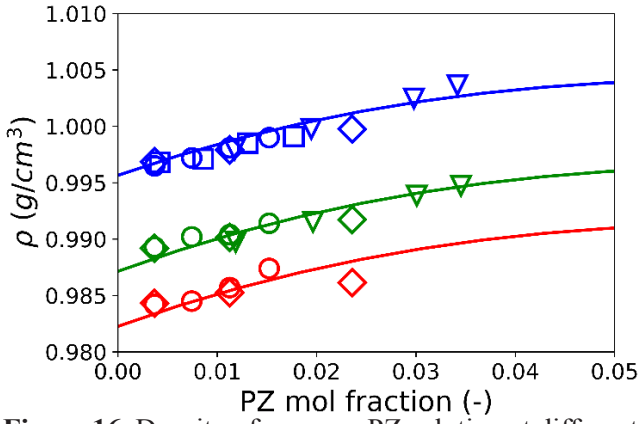

Figure 16. Density of aqueous PZ solution at different temperatures. Experimental data from: (o, Samanta and Bandyopadhyay (2006)), (□, Sun et al. (2005)), (∇, Derks et al. (2005)) and (◊, Muhammad et al. (2009)). Model at 101.325 kPa and: (-, blue) 303.15 K, (-, green) 323.15 K and (-, red) 333.15 K.

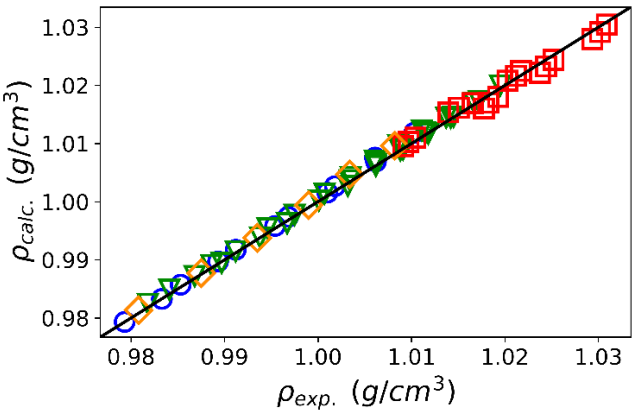

Figure 17. Density parity plot of aqueous MEA-MDEA solution at different temperatures and concentrations. Experimental data from: (o, Li and Lie (1994)), (□, Hagewiesche et al. (1995)), (5, Li and Shen (1992)) and (◊, Hsu and Li (1997)).

H_2O-MDEA-PZ

The parameters previously estimated for H_2O, MDEA and PZ systems were used in the optimization of the H_2O-MDEA-PZ system. Again, only four parameters were estimated and the results are given in Table 4. Figure 18 shows the parity plot for the density of the H_2O-MDEA-PZ system. It is seen that this

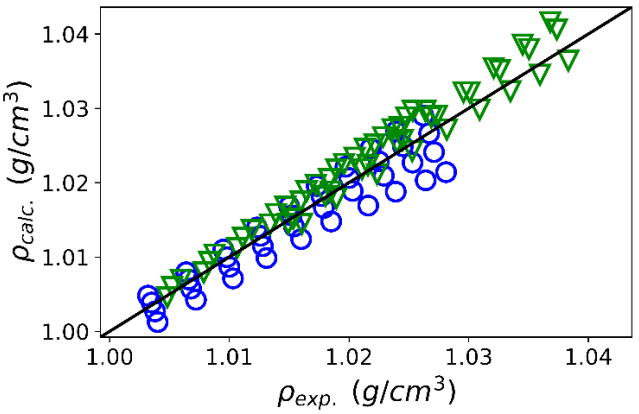

Figure 18. Density parity plot of aqueous MDEA-PZ solution at different temperatures and concentrations. Experimental data from: (o, Paul and Mandal (2006)), (∇, Muhammad et al. (2009)).

system is calculated with a little more deviation than the H_2O-MDEA-PZ as the points slightly deviate from the diagonal line. This is also seen in the calculated deviations. However, this deviation is still small (< 0.3 %) for engineering calculations and the model is considered good to predict the density of this ternary system. The best set of parameters was found with α_{ij} = 0.2.

CONCLUSIONS

In this work a new temperature and pressure dependency function for the Z_{RA} parameter of the modified Rackett equation was proposed. The model is able to accurately represent the densities of pure liquids. For pure water, there is a deviation at low temperatures (close to the melting point). However, the calculated deviations were below 1% for atmospheric pressure measurements and are considered negligible. For the pure amine, the deviations (AARD) were below 0.09%.

A model based on the NRTL model was also proposed for calculating the density of liquid mixtures. The model provides a more direct way to calculate the density of the systems as the number of parameters is not dependent on a polynomial. Seven aqueous systems (5 binaries and 2 ternaries) were tested in this work. The model is able to accurately predict the density of the binary and ternary systems tested in this work. With a few exceptions, the calculated deviations were below 0.09%, and below 0.2%, respectively, for the pure component system and aqueous solutions tested in this work.

ACKNOWLEDGEMENT

This work is supported by the Research Council of Norway through the CLIMIT program (Project No. 239789, Project: 3rd generation membrane contactor). In this work, Matplotlib (Hunter, 2007) was used to generate the figures.

NOMENCLATURE

a, A	Fitting parameter
AAD	Absolute average deviation, kg/m^3
AARD	Absolute average relative deviation, %
AMP	2-Amino-2-methyl-1-propanol
b, B	Fitting parameter
c, C	Fitting parameter
DEA	Diethanolamine
G_{ij}	NRTL coefficient
i, j	Component index
MAD	Maximum absolute deviation, kg/m^3
MEA	Monoethanolamine
MDEA	Methyldiethanolamine
MW	Molecular weight, kg/mol
NC	Number of components
NRTL	Non-Random Two-Liquid
p_c	Critical pressure, Pa
p_r	Reduced pressure, Pa/Pa
PZ	Piperazine
R	Dimensionless parameter
T	Temperature, K
T_c	Critical temperature, K
T_r	Reduced temperature, K/K
$\overline{V^E}$	Excess molar volumes, m^3/mol
$\overline{V^m}$	Molar volumes of mixture, m^3/mol
$\overline{V_i^0}$	Molar volumes of pure component i, m^3/mol
$\overline{V_i}$	Molar volumes of saturated liquids, m^3/mol
x	Mol fraction
Z_{RA}	Rackett compressibility factor
α_{ij}	Non-randomness parameter
ρ	Density, kg/m^3
τ_{ij}	NRTL coefficient

REFERENCES

Abrams, D.S., Prausnitz, J.M. Statistical thermodynamics of liquid mixtures: A new expression for the excess gibbs energy of partly or completely miscible systems. AIChE Journal, 21, 116-128 (1975). https://doi.org/10.1002/aic.690210115

Alvarez, E., Cerdeira, F., Gomez-Diaz, D., Navaza, J.M. Density, speed of sound, isentropic compressibility, and excess volume of binary mixtures of 1-amino-2-propanol or 3-amino-1-propanol with 2-amino-2- methyl-1-propanol, diethanolamine, or triethanolamine from (293.15 to 323.15) K. Journal of Chemical & Engineering Data, 55, 2567-2575 (2010). https://doi.org/10.1021/je900739x

Àlvarez, E., Gómez-Díaz, D., La Rubia, M.D., Navaza, J.M. Densities and viscosities of aqueous ternary mixtures of 2-(methylamino)ethanol and 2-(ethylamino)ethanol with diethanolamine, triethanolamine, N-methyldiethanolamine, or 2-amino-1-methyl-1-propanol from 298.15 to 323.15 K. Journal of Chemical & Engineering Data, 51, 955-962 (2006). https://doi.org/10.1021/je050463q

Amundsen, T.G., Øi, L.E., Eimer, D.A. Density and viscosity of monoethanolamine + water + carbon dioxide from (25 to 80) ◦ c. Journal of Chemical & Engineering Data, 54, 3096-3100 (2009). https://doi.org/10.1021/je900188m

Bernhardsen, I.M., Krokvik, I.R., Perinu, C., Pinto, D.D., Jens, K.J., Knuutila, H.K. Influence of pKa on solvent performance of MAPA promoted tertiary amines. International Journal of Greenhouse Gas Control, 68, 68-76 (2018). https://doi.org/10.1016/j.ijggc.2017.11.005

Campbell, S.W., Thodos, G. Saturated liquid densities of polar and nonpolar pure substances. Industrial & Engineering Chemistry Fundamentals, 23, 500-510 (1984). https://doi.org/10.1021/i100016a021

Chan, C., Maham, Y., Mather, A., Mathonat, C. Densities and volumetric properties of the aqueous solutions of 2-amino-2-methyl-1-propanol, n-butyldiethanolamine and n-propylethanolamine at temperatures from 298.15 to 353.15 K. Fluid Phase Equilibria, 198, 239-250 (2002). https://doi.org/10.1016/S0378-3812(01)00768-3

Chowdhury, F.I., Akhtar, S., Saleh, M.A. Densities and excess molar volumes of aqueous solutions of some diethanolamines. Physics and Chemistry of Liquids, 47, 638-652 (2009). https://doi.org/10.1080/00319100802620538

Derks, P.W., Hogendoorn, K.J., Versteeg, G.F. Solubility of N_2O in and density, viscosity, and surface tension of aqueous piperazine solutions. Journal of Chemical & Engineering Data, 50, 1947-1950 (2005). https://doi.org/10.1021/je050202g

Gao, H., Gao, G., Liu, H., Luo, X., Liang, Z., Idem, R.O. Density, viscosity, and refractive index of aqueous CO_2 -loaded and -unloaded ethylaminoethanol (EAE) solutions from 293.15 to 323.15 K for post combustion CO_2 capture. Journal of Chemical & Engineering Data, 62, 4205-4214 (2017). https://doi.org/10.1021/acs.jced.7b00586

Gunberg, L., Nissan, A.H. Mixture law for viscosity. Nature, 164, 799-800 (1949). https://doi.org/10.1038/164799b0

Hagewiesche, D.P., Ashour, S.S., Sandall, O.C. Solubility and diffusivity of nitrous oxide in ternary mixtures of water, monoethanolamine and N-methyldiethanolamine and solution densities and viscosities. Journal of Chemical & Engineering Data, 40, 627-629 (1995). https://doi.org/10.1021/je00019a020

Han, J., Jin, J., Eimer, D.A., Melaaen, M.C. Density of water (1) + diethanolamine (2) + CO_2 (3) and water (1) + n-methyldiethanolamine (2) + CO_2 (3) from (298.15 to 423.15) K. Journal of Chemical & Engineering Data, 57, 1843-1850 (2012a). https://doi.org/10.1021/je300345m

Han, J., Jin, J., Eimer, D.A., Melaaen, M.C. Density of water (1) + monoethanolamine (2) + CO_2 (3) from (298.15 to 413.15) K and surface tension of water (1) + monoethanolamine (2) from (303.15 to 333.15) K. Journal of Chemical & Engineering Data, 57, 1095-1103 (2012b). https://doi.org/10.1021/je2010038

Hawrylak, B., Burke, S.E., Palepu, R. Partial molar and excess volumes and adiabatic compressibilities of binary mixtures of ethanolamines with water. Journal of Solution Chemistry, 29, 575-594 (200). https://doi.org/10.1021/je0201119

Henni, A., Hromek, J.J., Tontiwachwuthikul, P., Chakma, A. Volumetric properties and viscosities for aqueous amp solutions from 25 ºC to 70 ºC. Journal of Chemical & Engineering Data, 48, 551-556 (2003). https://doi.org/10.1021/je0201119

Hsu, C.H., Li, M.H. Densities of aqueous blended amines. Journal of Chemical & Engineering Data, 42, 502-507 (1997). https://doi.org/10.1021/je960356j

Hunter, J.D. Matplotlib: A 2D graphics environment. Computing In Science & Engineering, 9, 90-95 (2007). https://doi.org/10.1109/MCSE.2007.55

Knudsen, J., Vilhemsen, P.J., Jensen, J., Biede, O. First year operating experience with a 1 t/h CO_2 absorption pilot plant at Esbjerg coal-fired power plant. Proceedings of European Congress of Chemical Engineering (ECCE-6), 3, 57-61. Copenhagen, 16-20 September 2007.

Knudsen, J.N., Jensen, J.N., Vilhelmsen, P.J., Biede, O. Experience with CO_2 capture from coal flue gas in pilot-scale: Testing of different amine solvents. Energy Procedia, 1, 783-790 (2009). https://doi.org/10.1016/j.egypro.2009.01.104

Kvamsdal, H.M., Haugen, G., Svendsen, H.F., Tobiesen, A., Mangalapally, H., Hartono, A., Mejdell, T. Modelling and simulation of the Esbjerg pilot plant using the CESAR 1 solvent. Energy Procedia 4, 1644-1651 (2011). http://dx.doi.org/10.1016/j.egypro.2011.02.036

Li, M.H., Lie, Y.C. Densities and viscosities of solutions of monoethanolamine + n-methyldiethanolamine + water and monoethanolamine + 2-amino-2-methyl-1-propanol + water. Journal of Chemical & Engineering Data, 39, 444-447 (1994). https://doi.org/10.1021/je00015a009

Li, M.H., Shen, K.P. Densities and solubilities of solutions of carbon dioxide in water + monoethanolamine + n-methyldiethanolamine. Journal of Chemical & Engineering Data, 37, 288-290 (1992). https://doi.org/10.1021/je00007a002

Liebenthal, U., Pinto, D.D.D., Monteiro, J.G.M.S., Svendsen, H.F., Kather, A. Overall process analysis and optimisation for CO_2 capture from coal fired power plants based on phase change solvents forming two liquid phases. Energy Procedia, 37, 1844-1854 (2013). http://dx.doi.org/10.1016/j.egypro.2013.06.064

Maham, Y., Liew, C.N., Mather, A. Viscosities and excess properties of aqueous solutions of ethanolamines from 25 to 80ºC. Journal of Solution Chemistry, 31, 743-756 (2002). http://dx.doi.org/10.1023/A:1021133008053

Maham, Y., Teng, T.T., Hepler, L.G., Mather, A.E. Densities, excess molar volumes, and partial molar volumes for binary mixtures of water with monoethanolamine, diethanolamine, and triethanolamine from 25 to 80ºC. Journal of Solution Chemistry, 23, 195-205 (1994). http://dx.doi.org/10.1007/BF00973546

Maham, Y., Teng, T.T., Mather, A.E., Hepler, L.G. Volumetric properties of (water + diethanolamine) systems. Canadian Journal of Chemistry, 73, 1514-1519 (1995). http://dx.doi.org/10.1139/v95-187

Mokraoui, S., Valtz, A., Coquelet, C., Richon, D. Volumetric properties of the isopropanolamine-water mixture at atmospheric pressure from 283.15 to 353.15 K. Thermochimica Acta, 440, 122-128 (2006). https://doi.org/10.1016/j.tca.2005.10.007

Monteiro, J.G.S., Pinto, D.D., Zaidy, S.A., Hartono, A., Svendsen, H.F. VLE data and modelling of aqueous N,N-diethylethanolamine (DEEA) solutions. International Journal of Greenhouse Gas Control, 19, 432-440 (2013). http://dx.doi.org/10.1016/j.ijggc.2013.10.001

Muhammad, A., Mutalib, M.I.A., Murugesan, T., Shafeeq, A. Thermophysical properties of aqueous piperazine and aqueous (N-methyldiethanolamine + piperazine) solutions at temperatures (298.15 to 338.15) K. Journal of Chemical & Engineering, Data 54, 2317-2321 (2009). http://dx.doi.org/10.1021/je9000069

Paul, S., Mandal, B. Density and viscosity of aqueous solutions of (N-methyldiethanolamine + piperazine) and (2-amino-2-methyl-1-propanol + piperazine) from (288 to 333) K. Journal of Chemical & Engineering Data, 51, 1808-1810 (2006). http://dx.doi.org/10.1021/je060195b

Pinto, D.D., Johnsen, B., Awais, M., Svendsen, H.F., Knuutila, H.K. Viscosity measurements and modeling of loaded and unloaded aqueous solutions of MDEA, DMEA, DEEA and MAPA. Chemical Engineering Science, 171, 340-350 (2017). https://doi.org/10.1016/j.ces.2017.05.044

Pinto, D.D., Knuutila, H., Fytianos, G., Haugen, G., Mejdell, T., Svendsen, H.F. CO_2 post combustion capture with a phase change solvent. pilot plant campaign. International Journal of Greenhouse Gas Control, 31, 153-164 (2014a). https://doi.org/10.1016/j.ijggc.2014.10.007

Pinto, D.D., Monteiro, J.G.M.S., Bersås, A., Haug-Warberg, T., Svendsen, H.F. eNRTL parameter fitting procedure for blended amine systems: MDEA-PZ case study. Energy Procedia, 37, 1613-1620 (2013). http://dx.doi.org/10.1016/j.egypro.2013.06.037

Pinto, D.D., Monteiro, J.G.S., Johnsen, B., Svendsen, H.F., Knuutila, H. Density measurements and modelling of loaded and unloaded aqueous solutions of MDEA (N-methyldiethanolamine), DMEA (N,N-dimethylethanolamine), DEEA (diethylethanolamine) and MAPA (N-methyl-1,3-diaminopropane). International Journal of Greenhouse Gas Control, 25, 173-185 (2014b). http://dx.doi.org/10.1016/j.ijggc.2014.04.017

Pinto, D.D., Svendsen, H.F. An excess Gibbs free energy based model to calculate viscosity of multicomponent liquid mixtures. International Journal of Greenhouse Gas Control, 42, 494-501 (2015). http://dx.doi.org/10.1016/j.ijggc.2015.09.003

PubChem. https://pubchem.ncbi.nlm.nih.gov/compound/11807#section=melting-point. Website accessed on 02/02/2018 (2018a).

PubChem. https://pubchem.ncbi.nlm.nih.gov/compound/piperazine#section=boiling-point. Website accessed on 02/02/2018 (2018b).

Rayer, A.V., Kadiwala, S., Narayanaswamy, K., Henni, A. Volumetric properties, viscosities, and refractive indices for aqueous 1-amino-2-propanol (monoisopropanolamine (MIPA)) solutions from (298.15 to 343.15) K. Journal of Chemical & Engineering Data, 55, 5562-5568 (2010). http://dx.doi.org/10.1021/je100300s

Razi, N., Bolland, O., Svendsen, H. Review of design correlations for CO2 absorption into mea using structured packings. International Journal of Greenhouse Gas Control, 9, 193-219 (2012). https://doi.org/10.1016/j.ijggc.2012.03.003

Redlich, O., Kister, A.T. Algebraic representation of thermodynamic properties and the classification of solutions. Industrial & Engineering Chemistry, 40, 345-348 (1948). http://dx.doi.org/10.1021/ie50458a036

Renon, H., Prausnitz, J.M. Local compositions in thermodynamic excess functions for liquid mixtures. AIChE Journal, 14, 135-144 (1968). http://dx.doi.org/10.1002/aic.690140124

Samanta, A., Bandyopadhyay, S.S. Density and viscosity of aqueous solutions of piperazine and (2-amino-2-methyl-1-propanol + piperazine) from 298 to 333 K. Journal of Chemical & Engineering Data, 51, 467-470 (2006). http://dx.doi.org/10.1021/je050378i

Sun, W.C., Yong, C.B., Li, M.H. Kinetics of the absorption of carbon dioxide into mixed aqueous solutions of 2-amino-2-methyl-l-propanol and piperazine. Chemical Engineering Science, 60, 503-516 (2005). https://doi.org/10.1016/j.ces.2004.08.012

Vetere, A. Again the rackett equation. The Chemical Engineering Journal, 49, 27-33 (1992). https://doi.org/10.1016/0300-9467(92)85021-Z

Wagner, W., Pruÿ, A. The IAPWS formulation 1995 for the thermodynamic properties of ordinary water substance for general and scientific use. Journal of Physical and Chemical Reference Data, 31, 387-535 (2002). http://dx.doi.org/10.1063/1.1461829

Wilson, G.M. Vapor-liquid equilibrium. XI. a new expression for the excess free energy of mixing. Journal of the American Chemical Society, 86, 127-130 (1964). http://dx.doi.org/10.1021/ja01056a002

Xu, S., Otto, F.D., Mather, A.E. Physical properties of aqueous AMP solutions. Journal of Chemical & Engineering Data, 36, 71-75 (1991). http://dx.doi.org/10.1021/je00001a021

Yang, F., Wang, X., Liu, Z. Volumetric properties of binary and ternary mixtures of bis(2-hydroxyethyl) amine with water, methanol, ethanol from (278.15 to 353.15) K. Thermochimica Acta, 533, 1-9 (2012). https://doi.org/10.1016/j.tca.2012.01.007

Yaws. Yaws' Critical Property Data for Chemical Engineers and Chemists. Knovel (2012).

Zhang, F.Q., Li, H.P., Dai, M., Zhao, J.P., Chao, J. Volumetric properties of binary mixtures of water with ethanolamine alkyl derivatives. Thermochimica Acta, 254, 347-357 (1995). https://doi.org/10.1016/0040-6031(94)02127-A